Beyond Mean-Field Calculation For Pairing Correlation

G. Hupin, D. Lacroix

April 26, 2012

Disclaimer

This document was prepared as an account of work sponsored by an agency of the United States government. Neither the United States government nor Lawrence Livermore National Security, LLC, nor any of their employees makes any warranty, expressed or implied, or assumes any legal liability or responsibility for the accuracy, completeness, or usefulness of any information, apparatus, product, or process disclosed, or represents that its use would not infringe privately owned rights. Reference herein to any specific commercial product, process, or service by trade name, trademark, manufacturer, or otherwise does not necessarily constitute or imply its endorsement, recommendation, or favoring by the United States government or Lawrence Livermore National Security, LLC. The views and opinions of authors expressed herein do not necessarily state or reflect those of the United States government or Lawrence Livermore National Security, LLC, and shall not be used for advertising or product endorsement purposes.

Beyond mean-field calculation for pairing correlation

Guillaume Hupin[1, 2, *] and Denis Lacroix[1, †]

[1]*Grand Accélérateur National d'Ions Lourds (GANIL),
CEA/DSM-CNRS/IN2P3, Bvd Henri Becquerel, 14076 Caen, France*
[2]*Lawrence Livermore National Laboratory, P. O. Box 808, L-414, Livermore, California 94551, USA*

The recently proposed Symmetry-Conserving Energy Density Functional approach [G. Hupin, D. Lacroix and M. Bender, Phys. Rev. C84, 014309 (2011)] is applied to perform Variation After Projection onto good particle number using Skyrme interaction including density dependent terms. Systematic study of the Kr and Sn isotopic chain is made. This approach leads to non-zero pairing in magic nuclei and a global enhancement of the pairing gap is obtained compared to the original theory that breaks the particle number symmetry. The need to consistently readjust the pairing effective interaction strength is discussed.

I. INTRODUCTION

The nuclear Energy Density Functional (EDF) is a versatile approach [1, 2] that allows one to describe a variety of phenomena in nuclei ranging from nuclear structure effects, nuclear dynamics, to thermodynamics. One specificity of nuclear energy functional approaches is that the densities used in the energy might not respect some of the properties related to the symmetry of the underlying bare many-body Hamiltonian [3, 4]. This is done by introducing a reference Slater (or quasi-particle) state from which the one-body normal density (and eventually the anomalous density) is constructed to express the energy. These densities are generally localized in space and therefore do not correspond to a translationally invariant system. This is often broadened to states that are neither an eigenstate of the particle number operator (then breaking the U(1) symmetry) nor of the total angular momentum operator.

The use of Symmetry-Breaking (SB)-EDF is a powerful technique to describe some aspects of nuclei like the onset of pairing and/or the onset of deformation. First however, restoration of broken symmetries is necessary to compare with experiments where eigenstates with good quantum numbers are probed. Second, the restoration of symmetries and more generally the use of configuration mixing techniques is a way to grasp some additional correlations associated with quantum fluctuations in a collective space[5, 6]. Ultimately, the state of the art of EDF is to perform a configuration mixing to describe the coexistence of different intrinsic configurations like shapes, excited states, electromagnetic and nuclear transitions.

This technique of symmetry breaking followed by symmetry restoration has been recently shown to lead to spurious contributions to the energy and must be ap-

plied with caution [7, 8]. Overall, the very notion of symmetry-breaking in a functional approach needs to be clarified [9]. For detailed discussion, see recent works [7, 8, 10–13]. Facing these difficulties, at present, three strategies have been proposed to perform well converged configuration mixing calculations within EDF: (i) One can eventually derive the energy functional starting from a true Hamiltonian and completely incorporate the Pauli principle [7]. (ii) For some specific functionals, by comparing with the Hamiltonian case, spurious contributions can be identified and removed from the energy functional [10–12] (iii) the energy functional used in the SB case can be consistently extended to a functional of the densities of the state with the symmetries restored. This is the Symmetry-Conserving (SC)-EDF approach proposed in ref. [14].

The strategies (i) and (ii) prevent us from using density dependent interactions with non-integer powers of the density, and strongly reduce the ability to tailor the density functional. Note that strategy (i) is nowadays used with the Gogny force [15–17] taking a specific care of the density dependent term. Recent applications of strategy (ii) have shown that this approach becomes rather involved when several symmetries are restored simultaneously[18]. While momentarily formulated only for the particle number restoration case (see also discussion in ref. [19]), the strategy (iii) can be used for any functional form like those used in the SB case starting from the Gogny or Skyrme like interaction, while having a different interaction in the pairing channel. Secondly, it is not required to strictly enforce the anti-symmetrization and some useful numerical approximations like the Slater approximation for the Coulomb exchange can still be used.

In this article, the work presented in ref. [14] is extended to perform Variation After Projection (VAP) enforcing good particle number. We show that the SC-EDF used with the up-to-date functionals based on Skyrme interaction can be competitive to describe pairing in nuclei.

───────

*Electronic address: hupin1@llnl.gov
†Electronic address: lacroix@ganil.fr

II. THE SYMMETRY-CONSERVING EDF APPROACH

Starting, from a quasi-particle state $|\Phi_0\rangle$, most currently used Symmetry-Breaking EDF based on the Skyrme[20] or Gogny[21] forces can be written as

$$\mathcal{E}_{\text{SB}}[\Phi_0] = \sum_i t_{ii} \, \rho_{ii} + \frac{1}{2} \sum_{i,j} \overline{v}^{\rho\rho}_{ijij} \, \rho_{ii}\rho_{jj}$$
$$+ \frac{1}{4} \sum_{i,j} \overline{v}^{\kappa\kappa}_{i\bar{i}j\bar{j}} \, \kappa^*_{i\bar{i}}\kappa_{j\bar{j}} \,, \qquad (1)$$

where $\overline{v}^{\rho\rho}$ and $\overline{v}^{\kappa\kappa}$ denote the effective vertices in the particle-hole and particle-particle channels. Here ρ and κ denote the normal and anomalous densities expressed in the canonical basis.

In the Hamiltonian case, the U(1) symmetry restoration can be made by considering the component of the quasi-particle state with specific particle number. Introducing the particle number projector P^N, a new state $|\Psi_N\rangle$ defined through:

$$|\Psi_N\rangle = P^N|\Phi_0\rangle \,. \qquad (2)$$

While there is no ambiguity when a Hamiltonian is used, the main challenge within EDF is to properly extend (1) to account for particle number conservation.

This problem has been carefully analyzed in ref. [14] leading to a generalization of the energy density functional given by:

$$\mathcal{E}_{\text{SC}}[\hat{\rho}^N, \hat{R}^N] = \sum_i t_{ii} \, \rho^N_{ii} + \frac{1}{2} \sum_{i\neq j, j\neq \bar{i}} \overline{v}^{\rho\rho}_{ijij} \, R^N_{jiji}$$
$$+ \frac{1}{2} \sum_i (\overline{v}^{\rho\rho}_{iiii} + \overline{v}^{\rho\rho}_{i\bar{i}i\bar{i}}) \, (\rho^N_{ii})^2$$
$$+ \frac{1}{4} \sum_{i\neq j, i\neq \bar{j}} \overline{v}^{\kappa\kappa}_{i\bar{i}j\bar{j}} \, R^N_{jj\bar{i}\bar{i}}$$
$$+ \frac{1}{2} \sum_i \overline{v}^{\kappa\kappa}_{i\bar{i}i\bar{i}} \, \rho^N_{ii} \, (1 - \rho^N_{ii}) \,, \qquad (3)$$

where ρ^N and R^N denote respectively the one and two bod matrices of the projected state, Eq. (2). Note that, within SC-EDF, it is further postulated that any dependence of the effective vertices in terms of the SB density should be replaced by an equivalent dependence of the projected density. Doing so, the energy becomes a functional of the projected state degrees of freedom (DOF) only. In former applications of SC-EDF, the expression of the energy has been used in the Projection After Variation (PAV) scheme showing the absence of any pathologies observed previously even if density dependent interaction are used in the functional.

Here, the SC-EDF is applied to perform VAP. In this case, the energy should be minimized with respect to all possible variations of the projected state DOF, i.e.

$$\delta\mathcal{E}_{\text{SC}}[\hat{\rho}^N, \hat{R}^N] \, = \, 0. \qquad (4)$$

In the following we will consider the specific case where the state $|\Phi_0\rangle$ is written in a BCS form as

$$|\Phi_0\rangle \, = \, \prod_{i>0} \left(u_i + v_i \, a^\dagger_i a^\dagger_{\bar{i}} \right) |0\rangle \,, \qquad (5)$$

with $u^2_i + v^2_i = 1$. Accordingly, variation of the projected state DOF can be recast into variations of the single-particle state components $\phi_i(\mathbf{r})$ associated to the creation operator $a^\dagger_i$ and variations of the quantity v^2_i corresponding to the SB occupancy of orbital i. We then end up with a set of coupled equation:

$$\frac{\delta\mathcal{E}_{\text{SC}}}{\delta\phi^\star_i(\mathbf{r})} \, = \, 0, \qquad \frac{\delta\mathcal{E}_{\text{SC}}}{\partial v^2_i} = 0 \qquad (6)$$

to be solved self-consistently. This procedure is the same as the one generally used in the Hamiltonian case in PNP-VAP [22–24]. The eigenvalue equations of the self-consistent problem are recalled and explained in Appendix A. It is worth mentioning that we took advantage of the analytic expressions of the densities R^N[25]. This step is crucial to reduce the computational burden of the calculation.

The Euler-Lagrange equations associated with the minimization of the energy yield respectively to a set of eigenvalues and non-linear equations that are rather involved numerically. Taking advantage of the EDF flexibility without breaking the consistency requirement of the approach [14], the minimization can be greatly simplified numerically by making the assumption in Eq. (3) that,

$$R^N_{jiji} \, \simeq \, \rho^N_{ii}\rho^N_{jj} \,. \qquad (7)$$

This approximation is used below.

III. APPLICATIONS

The EV8 code of Bonche, Flocard and Heenen[26] has been updated to allow minimization of the functional (3) using the approximation in (7). The numerical method consists in solving the mean field problem by an imaginary time step method [27] and the optimization of the occupation probabilities by a sequential quadratic programming. In the following, the SC-EDF method is used with the SLy4 interaction in the mean-field channel [28] while the effective pairing interaction considered [29] is

$$v^{\kappa\kappa}(\mathbf{r}, \mathbf{r}') \, = \, \frac{V_0}{2} \, (1 - P_\sigma) \, \left(1 - \left(\frac{\rho(\mathbf{R})}{\rho_0}\right)^\alpha\right) \, \delta(\mathbf{r} - \mathbf{r}'), \qquad (8)$$

with $\mathbf{R} = (\mathbf{r} + \mathbf{r}')/2$. $V_0 = 1250$ MeV is the pairing constant, $\alpha = 1$ and $\rho_0 = 0.16$ fm^{-3} is the saturation density. In addition, to avoid the ultra-violet divergence that appears with contact interaction, a cut-off factor[30] with an energy interval of 5 MeV is used to select states

around the Fermi energy. These values have been typically used to reproduce neutron and proton separation energies[31] and, in the standard terminology, correspond to a surface pairing.

In this work, SC-EDF calculations are systematically performed for the Kr and Sn isotopic chains. In the latter case, the proton number is magic while in the former case it is not. As an illustration of the results, the evolution of the energy as a function of the deformation obtained with the SC functional (blue solid line) is compared to the original BCS result (green dashed line) for ^{72}Kr and ^{86}Kr respectively in panel (a) and (b) of figure 1. Similar curves are shown in figure 2 for ^{116}Sn and ^{132}Sn. These nuclei have been selected because they are representative of the different types of situations: mid-shell nucleus (^{72}Kr), simply (^{86}Kr and ^{116}Sn) or doubly magic nucleus (^{132}Sn). The results have been obtained by adding a quadrupole constraint in the minimization while the deformation parameter is defined by

$$\beta = \sqrt{\frac{5}{16\pi}} \frac{4\pi}{3R^2 A} \langle Q_{20} \rangle, \qquad (9)$$

where $\langle Q_{20} \rangle$ is the quadrupole deformation and $R = 1.2 \ A^{1/3}$ is the nuclear radius. It can be seen in fig-
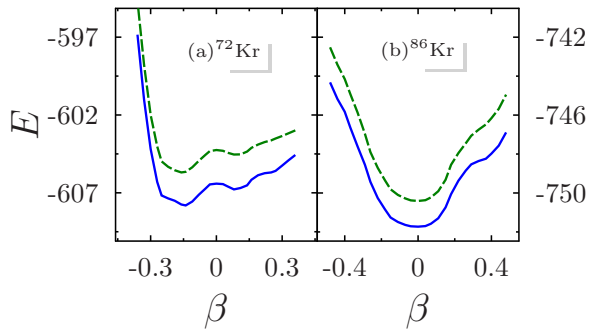

FIG. 1: (Color online) Evolution of the energy obtained using the VAP calculation (blue solid line) for the ^{72}Kr (a) and ^{86}Kr (b) as a function of deformation. In each case, the BCS result obtained with the original EV8 code is shown with a green dashed curve.

ures 1 and 2, that the potential energy curves obtained with the SC-EDF are smooth and, as already discussed in ref. [14], we do not see any of the pathologies observed in other approaches with density dependent interactions [8, 11].

Figures 2 and 1 illustrate that the energy potential curves of the SC-EDF functional with respect to the quadrupole deformation are shifted from BCS. There are no changes in the shape of these curves, both BCS and shifted SC functional can be almost superimposed. The energy gain, illustrated by the shift, is between 1 and 2 MeV for mid-shell and simply magic nuclei while the doubly magic nuclei ^{132}Sn gains more than 0.5 MeV. This increase in correlation energy comes from the improved
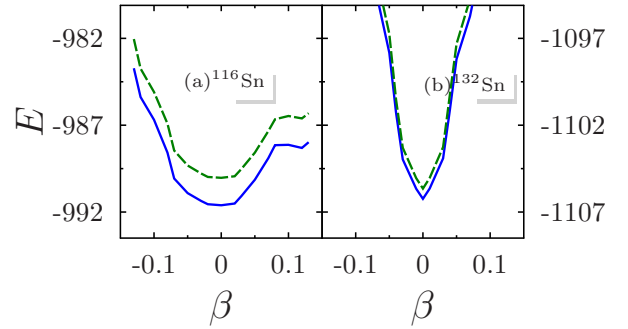

FIG. 2: (Color online) Same as figure 1 for the ^{116}Sn (a) and ^{132}Sn (b).

treatment of the pairing correlations from the projection formalism that has been used to tailor the functional dependances of the energy.

As seen from figures 2 and 1, the full SC functional induces rather small differences on the total energy compared to the original BCS case. It should be mentioned however that the pairing energy is always enhanced when the symmetry is conserved, especially around shell closures, as expected. Indeed, when the pairing is treated within BCS or HFB, there is a sudden disappearance of correlations in the weak pairing regime, this is the well-known BCS threshold anomaly. A measure of the pairing strength is provided by the mean gap[32]:

$$\overline{\Delta}_{n/p} = \frac{E_{\text{pairing}}^{n/p}}{\sum_i \sqrt{\rho_{ii}(1-\rho_{ii})}}, \qquad (10)$$

where ρ_{ii} are the occupation probabilities of a given theory and $E_{\text{pairing}}^{n/p}$ its neutron/proton pairing energy. In the SC-EDF, these energies are calculated as the sum of the last two terms in Eq. (3). This observable has the advantages (i) to correlate with the pairing gap in the limit of a constant pairing interaction (ii) to probe both the pairing energy and the trend of the occupation probabilities such as the fragmentation of occupation numbers around the Fermi surface.

In figures 3 and 4, the deformation parameter β (Eq. 9) at the minimum of the energy (3a and 4a), the average proton (3b and 4b) and neutron (3c and 4c) gaps are shown as a function of the neutron number along the Kr and Sn isotopic chain respectively. The BCS (green dashed lines) and the SC-EDF (blue solid lines) results are compared. Note that consistently with the observations from figures 1 and 2, the deformation parameter at the minimum of the energy (long dashed line) is the same for both BCS and SC-EDF, hence is plotted once. In this figure, BCS exhibits strong variations of the gap close to the $N = 50$ shell closure. This is a fingerprint of the abrupt disappearance of pairing in this formalism close to magicity. It is also worth to keep in mind that the evolution of deformation as N increases might also induce local fluctuations. This is the case for $N > 56$ in
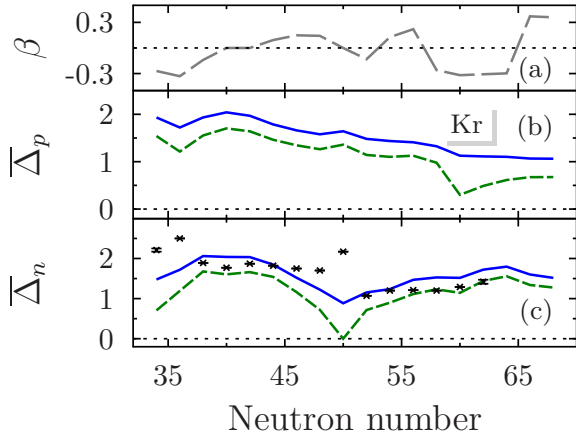
FIG. 3: (Color online) Value of the deformation parameter β (Eq. 9) at the minimum (a), average proton (b) and neutron (c) mean gaps defined by Eq. 10 are shown as a function of the neutron number along the Kr isotopic chain obtained from BCS (green dashed lines) and the SC-EDF (blue solid lines). The deformation parameter at the minimum is the same for both BCS and SC-EDF (gray long dashed line). The calculations are performed with a SLy4 effective interaction that includes a non-integer density dependence and a density dependent pairing interaction(Eq. (8)). The minimization is performed including the quadrupole degree of freedom. In the neutron case, the experimental gaps (black crosses) and their error bars[34] obtained with the three points formula(see [32, 33]) are also presented.
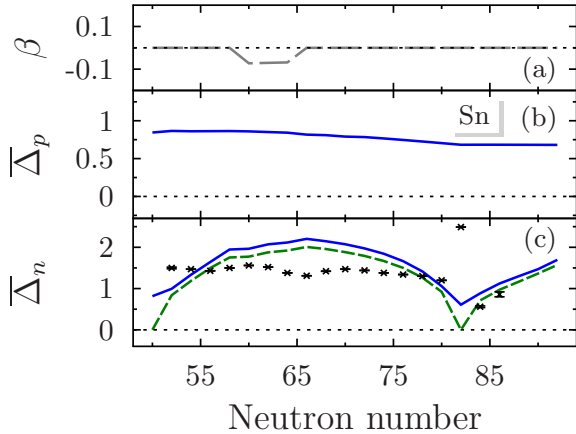

FIG. 4: (Color online) Same as figure 3 for the Sn isotopic chain. The proton mean gap (b) of BCS identifies with zero along the isotopic line.

the Kr chain as we can see from the evolution of the deformation (3a) reflected by variations in panels (3b) and (3c).

In the SC-EDF case, it is observed that the pairing gap is systematically enhanced compared to the BCS results. This enhancement is increased at the shell closure. For instance, in the proton gap of Sn isotopes, a mean gap of ~ 0.7 MeV is obtained (see figure 4) while it was

equal to zero at the BCS level. In the Kr isotopic chain, both BCS and SC-EDF lead to deformed nuclei with the same deformation parameter. The increase of pairing correlations is only due to a better treatment of quantum fluctuations in gauge space by the SC method. It is then seen that the increase at the shell closure ($N = 50$) is further enhanced to ~ 1 MeV while it is of the order of $0.3 - 0.5$ MeV in the mid-shell. Altogether, the pairing gap obtained within the VAP approach is much smoother than the BCS pairing gap and more consistent with the experimental observation.

It is important to note that the increase of the pairing gap is not fully reflected in the lowering of the ground state binding energy. Indeed, the SC-EDF is a fully self-consistent approach and when the enhanced pairing built up in the minimization, the mean-field reorganizes. Generally, it is observed that the mean-field energy, denoted by E_{MF} and defined as the total energy minus the pairing energy, increases slightly and partially compensates for the effect of the pairing. In figures 5 and 6, the three quantities

$$
\begin{aligned}
\Delta E_{\mathrm{pairing}} &= E_{\mathrm{pairing}}^{\mathrm{VAP}} - E_{\mathrm{pairing}}^{\mathrm{BCS}}, \\
\Delta E_{\mathrm{MF}} &= E_{\mathrm{MF}}^{\mathrm{VAP}} - E_{\mathrm{MF}}^{\mathrm{BCS}}, \\
\Delta E_{\mathrm{tot}} &= E_{\mathrm{tot}}^{\mathrm{VAP}} - E_{\mathrm{tot}}^{\mathrm{BCS}},
\end{aligned}
$$

are displayed as a function of the neutron number respectively from panel (a) to (c) for the Kr and Sn isotopes. In these figure, we see that $\Delta E_{\mathrm{pairing}}$ (5a and 6a) is always negative while ΔE_{MF} (5b and 6b) is always positive and therefore, the net reduction of the total energy (c) is much less than the pairing correlation would suggest.

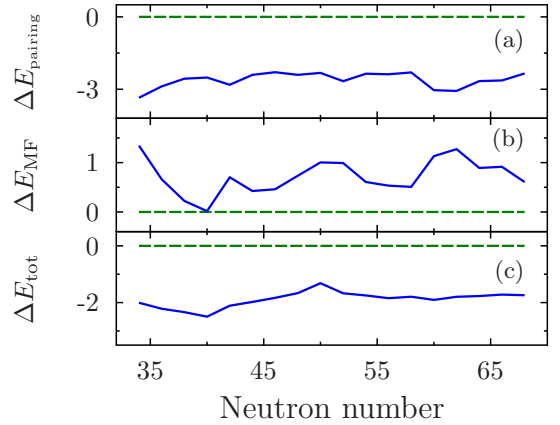Altogether, the total energy is shifted. The transition

FIG. 5: (Color online) Evolution of the quantities $\Delta E_{\mathrm{pairing}}$ (a), ΔE_{MF} (b) and ΔE_{tot} (c) along the Kr isotopic chain. The horizontal dashed line corresponds to the case where BCS and SC-EDF would be identical.

from a sharp Fermi distribution around single or doubly magic nuclei with BCS to a fragmented Fermi surface with non-zero pairing within SC-EDF leads to a significant change in the mean-field energy, especially due to
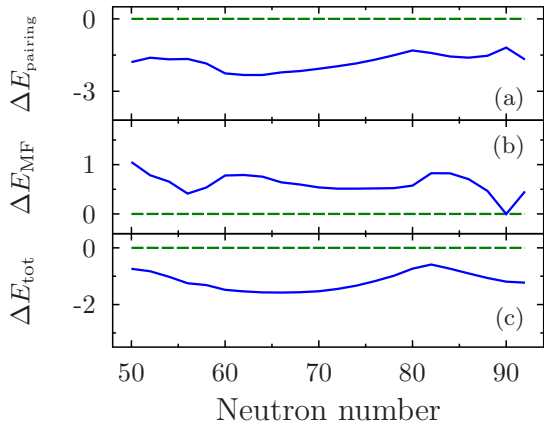
FIG. 6: (Color online) Same as figure 5 for the Sn isotopic chain.

the contribution of single-particle levels above the Fermi energy. We can observe on both figures 5 and 6 this effect. However, it is not possible to give more general trends because of the deformation and self-consistency of the theory.

In figure 7, the two neutron separation energies S_{2n} obtained in the BCS (green dashed line) and SC-EDF (blue solid line) are compared with the experimental values (black open circles). This quantity is sometime used in the literature to adjust the pairing effective interaction parameters. We see on the figure that both BCS and VAP are consistent with experiments. In fact, the S_{2n} are not affected by the variation after projection performed within SC-EDF.
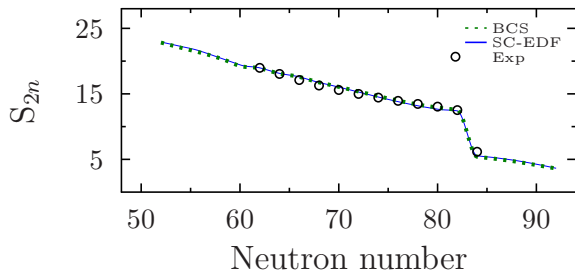

FIG. 7: (Color online) Comparaison of the two neutron separation energies S_{2n} along the Sn isotopic chain between BCS (green dotted line) and SC-EDF (blue solid line) with the experimental values (black open circles).

The applications of the SC-EDF functional show that the bulk properties (figures 1, 2 and 7) of the underlying effective interaction are conserved while the total binding and pairing energies are shifted (figures 5 and 6). For all nuclei studied, the SC-EDF functional predicts a non zero pairing energy and a fragmented Fermi surface. This is reflected by the non zero pairing gap (figures 3 and 4) for all nuclei including single and doubly magic

ones where BCS leads to a Fermi distribution for the orbital occupancies. In the following, the evolution of these observations are investigated as a function of the refitting of the strength V_0 of the pairing interaction.

IV. DISCUSSION OF THE PAIRING STRENGTH

The pairing interaction used above is often adjusted to properly describe pairing gaps in EDF using BCS or HFB especially in the mid-shell [32, 35–37]. As seen in the previous section, going beyond the mean-field leads to an overestimation of the pairing energy in this region. Consistently with a density functional approach, one should indeed *a priori* readjust the pairing strength when the functional changes. In this section, the results of VAP with an optimal value of the pairing strength are presented.
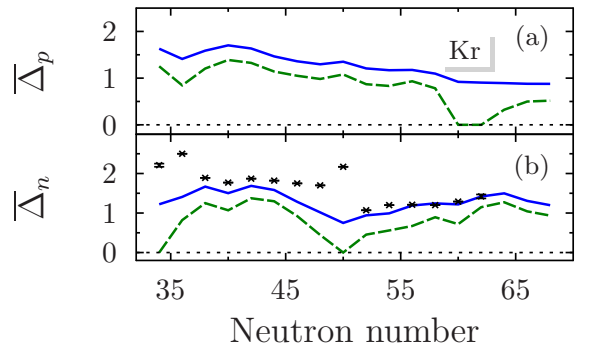

FIG. 8: (Color online) Same as figure 3 with a pairing strength of $V_0 = 1100$ MeV. The green dashed curve corresponds to the BCS result while the blue solid line corresponds to the SC-EDF case.
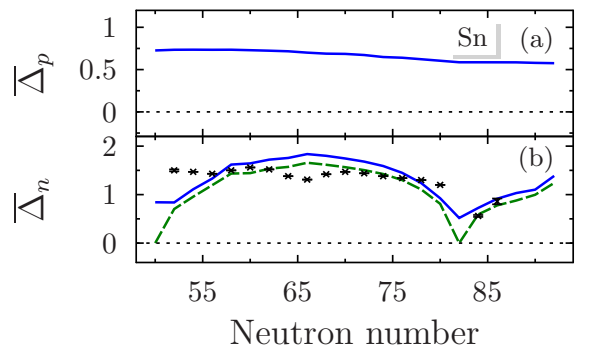

FIG. 9: (Color online) Same as figure 4 for the Sn isotopes.

In figures 8 and 9, results of the BCS (green dashed line) and SC-EDF (blue solid line) with a pairing strength $V_0 = 1100$ MeV are shown. This value of the strength has been chosen to properly describe Kr isotopes in the open-shell. By comparing these figures with 3 and 4, it

can be observed that SC-EDF with the reduced pairing interaction reproduces the original BCS result (with $V_0 = 1250$ MeV) in open shell nuclei.

It should however be mentioned that the refitting of pairing effective interaction solely when incorporating particle number projection is a too simplistic strategy to properly describe both the pairing and the bulk properties in nuclei. This is illustrated in Table I where the binding and pairing energies obtained with BCS and the original pairing interaction are compared with the SC-EDF results and the reduced pairing strength. While

TABLE I: Comparison between the binding and pairing energies of selected Kr isotopes predicted by BCS (with $V_0 = 1250$ MeV) and SC-EDF (with $V_0 = 1100$ MeV).

N	Z	BCS	BCS pairing	VAP	VAP pairing	Exp[34]
46	36	-715.64	-7.44	-716.34	-6.98	-714.27
48	36	-733.43	-5.19	-734.29	-5.44	-732.26
50	36	-750.41	-4.99	-750.91	-5.49	-749.23
52	36	-761.65	-5.04	-762.49	-5.47	-761.80
54	36	-772.3	-5.9	-773.18	-5.63	-773.21

pairing energies are similar, as could be anticipated from the fact that the gaps are similar, the binding energy deduced with the SC-EDF is often lower than the BCS and the original BCS is closer to the experimental binding energy. This stems from the fact that both the mean-field and pairing channel have been consistently adjusted simultaneously at the BCS level. When performing VAP not only the pairing correlations are affected but also additional correlations build up in the particle-hole channel, leading to a rather significant reorganization of the mean-field itself. This has been already clearly applied in figures 5 and 6. As a consequence, to improve the quality of theories that go beyond mean-field by restoring symmetries compared to those where symmetries are broken, in the near future, a complete readjustment of all components of the functional (mean-field and pairing) should be considered at the VAP level.

V. CONCLUSION

The recently proposed Symmetry-Conserving EDF approach to incorporate the effect of particle number conservation is performed in the Variation After Projection (VAP) scheme. The VAP is applied using density dependent interaction both in the mean-field and pairing chan-

nels. Such a density dependence, while impossible to use in configuration mixing calculations, does not lead to any difficulty in the SC-EDF framework. Systematic study of the krypton and tin isotopic chains is made showing the increase of pairing energy when particle number conservation is taken into account self-consistently. In particular, the description of correlations close or in the vicinity to closed shell nuclei is improved. Indeed, as expected, the symmetry conserving theory predicts non vanishing pairing gaps around and at shell closures. The present study clearly shows that the incorporation of symmetry restoration leads to an enriched functional and that the parameters used to design the functional in the original symmetry breaking approach need to be consistently readjusted. Here, a first attempt is made to reduce the pairing strength in order to properly describe pairing gaps. We point out that, ultimately, coefficients of the functional in both mean-field and pairing channels should be simultaneously optimized to really gain in predictive power of EDF approaches.

Appendix A: Euler-Lagrange equations

In the case of the SC-EDF built from a quasi-particle vacuum and a two-body delta interaction, the eigenequations to be solved as a self-consistent mean-field problem read

$$\frac{\partial \mathcal{E}_{\text{SC}}}{\partial \phi_i^\star(\mathbf{r})} = \Big(-\frac{\hbar^2}{2m^\star} \Delta + \sum_{j \neq (i,\bar{i})} \frac{\partial \bar{v}_{ijij}^{\rho\rho}}{\partial \phi_i^\star(\mathbf{r}) \partial \phi_i(\mathbf{r})} \frac{R_{jiji}^N}{\rho_{ii}^N} + \frac{\partial \bar{v}_{iiii}^{\rho\rho}}{\partial \phi_i^\star(\mathbf{r}) \partial \phi_i(\mathbf{r})} \rho_{ii}^N - \varepsilon_i \Big) \rho_{ii}^N \phi_i(\mathbf{r}), \quad (A1)$$

where the contribution from the pairing part of the functional have been neglected as it is usually done, $\bar{v}^{\rho\rho}$ is a particle-hole contact interaction, R_{jiji}^N is the projection of the one body density acting in the particle-hole channel and ε_i is the Lagrange multiplier that enforces the normalization of the single-particle state ϕ_i. It can be noted that in this form there is one potential for each orbitals due to the density dependence in the summation. The role of the prescription 7 is to remove this dependency hence recovering a single mean-field for all orbits.

[1] M. Bender, P.-H. Heenen and P.-G. Reinhard, Rev. Mod. Phys. **75**, 121 (2003).

[2] P. Ring and P. Schuck, The Nuclear Many-Body Problem (Springer-Verlag, 1980).

[3] P.-G. Reinhard, Nucl. Phys. A **420**, 173-192 (1984).
[4] W. Nazarewicz, Prog. Part. Nucl. Phys. **28**, 307-330 (1992).
[5] J. L. Egido and P. Ring, Nucl. Phys. A **383**, 189 (1982).
[6] J. L. Egido and P. Ring, Nucl. Phys. A **388**, 19 (1982).
[7] M. Anguiano, J.L. Egido, L.M. Robledo, Nucl. Phys. A **696**, 467 (2001).
[8] J. Dobaczewski, M. V. Stoitsov, W. Nazarewicz, and P.-G. Reinhard, Phys. Rev. C **76**, 054315 (2007).
[9] T. Duguet and J. Sadoudi, J. Phys. G **37**, 064009 (2010).
[10] M. Bender, T. Duguet, and D. Lacroix, Phys. Rev. C **79**, 044319 (2009).
[11] T. Duguet, M. Bender, K. Bennaceur, D. Lacroix, and T. Lesinski, Phys. Rev. C **79**, 044320 (2009).
[12] D. Lacroix, T. Duguet, and M. Bender, Phys. Rev. C **79**, 044318 (2009).
[13] L. M. Robledo, J. Phys. G **37**, 064020 (2010).
[14] G. Hupin, D. Lacroix, and M. Bender, Phys. Rev. C **84**, 014309 (2011).
[15] N. López Vaquero, T. R. Rodriguez, J. L. Egido, Phys. Lett. B**704**, 520 (2011); Phys. Lett. B**705**, 543(2011).
[16] T. R. Rodríguez and J. L. Egido, Phys. Rev. Lett. **99**, 062501 (2007).
[17] T. R. Rodríguez and J. L. Egido, Phys. Rev. C **81**, 064323 (2010).
[18] M. Bender et al, *in preparation*.
[19] G. Hupin and D. Lacroix proceeding of Ykis 2011 symposium to be published in Prog. Theor. Phys. Supplement (arXiv1203.3925)
[20] T. H. R. Skyrme, Nucl. Phys. **9**(4), 615-634 (1959).
[21] D. Gogny, P. Pires and D. R. Tourreil, Phys. Lett. B **32**(7), 591-595 (1970).
[22] J. A. Sheikh and P. Ring, Nucl. Phys. A **665**, 71 (2000).
[23] J. A. Sheikh, E. Lopes, and P. Ring, Phys. At. Nucl. **64**, 477(2001).
[24] K. Dietrich, H. J. Mang and J. H. Pradal, Phys. Rev. **135**, B22 (1964).
[25] D. Lacroix and G. Hupin, Phys. Rev. B **82**, 144509 (2010).
[26] P. Bonche, H. Flocard, and P.-H. Heenen, Comput. Phys. Commun. **171**, 49 (2005).
[27] K. T. R. Davies, H. Flocard, S. J. Krieger, and M. S. Weiss, Nucl. Phys. A **342**, 111-123 (1980).
[28] E. Chabanat, P. Bonche, P. Haensel, J. Meyer, R. Schaeffer, Nucl. Phys. A **635**, 231 (1998).
[29] R. R. Chasman, Phys. Rev. **C** 14, 1935-1945 (1976).
[30] P. Bonche, H. Flocard, P.-H. Heenen, S. J. Krieger, and M. S. Weiss, Nuc. Phys. A **443**, 3963 (1985).
[31] C. Rigollet, P. Bonche, H. Flocard, and P.-H. Heenen, Phys. Rev. C **59**, 3120-3127 (1999).
[32] J. Dobaczewski, H. Flocard, and J. Treiner, Nucl. Phys. A **422**, 103-139 (1984).
[33] T. Duguet, P. Bonche, P.-H. Heenen, and J. Meyer, Phys. Rev. C **65**, 014311 (2001).
[34] Data retrieved from the NNDC database, version of (03/04/2012), Online Data Service.
[35] J. Dobaczewski, W. Nazarewicz, and T. R. Werner, Phys. Scr. **T56**, 15-22 (1995).
[36] T. Lesinski, K. Bennaceur, T. Duguet, and J. Meyer, Phys. Rev. C **74**, (2006).
[37] J. Margueron, H. Sagawa, and K. Hagino, Phys. Rev. C **76**, 1-11 (2007).